J Radioanal Nucl Chem (2013) 298:1427–1434
DOI 10.1007/s10967-013-2607-7

Synthesis, characterization, and application of titanate nanotubes for Th(IV) adsorption

Jianliang Liu · Mingbiao Luo · Zizun Yuan · Aidong Ping

Received: 26 February 2013 / Published online: 17 July 2013

Abstract Titanate nanotubes (TNTs) have been synthesized by a hydrothermal method using rutile TiO_2 powder as titanium source. The determination of the structure and morphology was characterized by XRD, FTIR, SEM and TEM. The results indicate that the TNTs successfully synthesized under hydrothermal conditions of 150 °C. The adsorption of Th(IV) on TNTs was studied as a function of contact time, pH values, ionic strength, initial Th(IV) concentration and temperature under ambient conditions by using batch technique. The results indicate that adsorption of Th(IV) on TNTs is strongly dependent on pH values, but weakly dependent on ionic strength; Adsorption kinetics was better described by the pseudo-second-order model. The adsorption isotherms are simulated by Langmuir and Freundlich models well. $\Delta G°$, $\Delta H°$ and $\Delta S°$ free energy were calculated from experimental data, The results indicate that the adsorption of Th(IV) on TNTs is an endothermic and a spontaneous process, and increases with increasing temperature. The adsorption of Th(IV) on TNTs is mainly dominated by chemical sorption or surface complexation.

Keywords Titanate nanotubes · Th(IV) · Adsorption

Introduction

Thorium is a naturally radioactive element widely distributed over the earth's crust. It has been widely used in nuclear fuel industry, alloy, and laboratory investigations [1]. But thorium is long-lived radionuclides with a suite of radioactive daughter products which can pose a human health and ecosystems risk [2]. Therefore, the removal and recovery of thorium from contaminated water is an urgent and essential work. Various methods including chemical precipitation [3], solvent extraction [4], ion exchange [5] and adsorption [6–13] are effective methods to remove thorium from aqueous solution. Among these methods, adsorption is an efficient and convenient method because of its cost effective treatment, easy operation, no chemical reagents needed and no sludge produced [14]. Numerous adsorbents have been used for the removal of thorium from the aqueous solution, such as natural and modified clays [6], carbon materials [7, 8], biosorbents [9], molecular sieves [10], various resins [11] and other specific materials [12, 13].

Recently, Titanate nanotubes has attracted great interest in nuclear waste management because of their large surface area, more surface atom and the surface rich in hydroxyl groups [15]. TNTs not only have exhibited great potential for the adsorption of heavy metal ions Cu(II) [16], Ag(I) [17], Pb(II) [17, 18], Cd(II) [19], Cr(II) [19], As(III) [20], but also have showed high adsorption capacity in the removal of U(VI) [21], Eu(III) [22], ^{63}Ni(II) [23] from aqueous solution. However, the investigation of radionuclides adsorption on TNTs is still scarce, and the adsorption mechanism is still unclear.

Herein, the adsorption of Th(IV) on TNTs was investigated by using batch technique. The objectives of this work was: (1) synthesized and characterized the TNTs; (2) to study the effect of contact time, pH values, ionic strength and temperature on the Th(IV) adsorption on TNTs; (3) to describe Th(IV) adsorption isotherms with Langmuir and Freundlich models; (4) to calculate the thermodynamic

J. Liu · M. Luo (✉) · Z. Yuan · A. Ping
State Key Laboratory Breeding Base of Nuclear Resources and Environment, East China Institute of Technology, Nanchang 330013, People's Republic of China
e-mail: luomingbiao@yahoo.cn

parameters of Th(IV) adsorption, such as $\Delta G°$, $\Delta H°$ and $\Delta S°$; (5) to evaluate the adsorption mechanism of Th(IV) on TNTs.

Experimental

Reagents and apparatus

All chemical reagents used in the experiments were purchased as analytical reagent grade and used without any further purification. All solutions in this experiment were prepared using Milli-Q deionized water. The stock solution of Th(IV) (1 mg mL^{-1}) was prepared by dissolving 1.1895 g of $Th(NO_3)_4{\cdot}4H_2O$ in 30 mL (1+2) HCl, and then the solution was transferred into a 500 mL volumetric flask and diluted to the mark with Milli-Q deionized water to produce a Th(IV) stock solution. A 721-E spectrophotometer (Shanghai, China) was used for the determination of the Th(IV). pHS-3C (Shanghai, China) pH meter was used for pH adjustment. The FTIR spectra were carried out using a Nicolet 380 spectrophotometer in pressed KBr pellets (50 mg KBr and 1 mg of TNTs). X-ray powder diffractometry were carried out using an Shimadzu XRD-6000 diffractometer with Cu Kα radiation. Scanning electron microscopy (SEM) images were obtained with a JEOL JSM-6700F. Transmission electron microscopy (TEM) images were obtained with a JEOL JEM-2010.

Synthesis of TNTs

TNTs were synthesized via a hydrothermal method of 3 g rutile TiO_2 nanopowder was mixed with 120 mL 10 mol L^{-1} NaOH aqueous solution and stirred for 60 min at room temperature. Subsequently heated in a 200 mL Teflon-lined stainless steel autoclave at 150 °C for 48 h, then the reaction vessel was cooled to room temperature and subsequently washed by 0.1 M HCl aqueous solution and Milli-Q deionized water respectively until the pH of rinsing solution was approximately 7.0. The obtained precipitate was dried in a vacuum oven at 90 °C for 12 h and stored in glass bottles until used.

Batch sorption experiments

The adsorption experiments were carried out by batch technique in polyethylene centrifuge tubes under ambient conditions at 298.15 ± 2 K. The stock solution of TNTs and $NaClO_4$ were pre-equilibrated for 4 h before the addition of Th(IV) stock solution. The pH was adjusted to desired values by adding negligible volumes of 0.1 mol L^{-1} HCl or 0.1 mol L^{-1} NaOH to achieve the desired pH values. After equilibrium, the pH of the suspension was measured and the samples were centrifuged at 10000 rpm for 30 min to separate the solid and liquid phases. Then the supernatant solution was measured for residual Th(IV) concentration. The concentration of Th(IV) was analyzed by spectrophotometry at 660 nm by using Th(IV) Arsenazo(III) complex [11]. The blank experiments demonstrated that the adsorption of Th(IV) on the polyethylene tube walls was negligible. The amount of adsorbed Th(IV) and distribution coefficient (K_d) was estimated from the difference of the Th(IV) concentration in the aqueous before and after the adsorption.

$$q = (C_0 - C_e) \times \frac{V}{m} \quad (1)$$

$$K_d = \frac{V}{m}\left(\frac{C_0}{C_e} - 1\right) \quad (2)$$

where q (mg g^{-1}) is the amount of Th(IV) adsorbed on TNTs; C_0 (mg mL^{-1}) is the initial concentration of Th(IV) in the solution; C_e (mg mL^{-1}) is the concentration of Th(IV) in supernatant after centrifugation; m (g) is the mass of TNTs and V (mL) is the volume of aqueous solution.

Results and discussion

XRD analysis

The X-ray diffraction (XRD) pattern of the sample is shown in Fig. 1. The remarkable diffraction peaks at $2\theta = 10.5°$ is represented interlayer space of TNTs [22, 24], The peaks at $2\theta = 28.4°$, 24.3° and 48.3° is perhaps the structure of sodium titanate, indicating that the remnant Na^+ stabilized the nanotube structures [25].

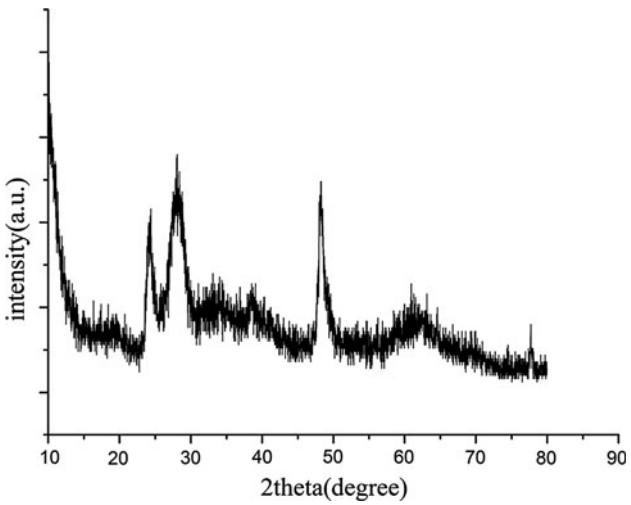

Fig. 1 XRD analysis of TNTs

FTIR analysis

Study of the as-synthesized TNTs was also followed by FTIR in the range between 4000 and 400 cm^{-1} and the results obtained have been illustrated in Fig. 2. Absorption peak at 400–800 cm^{-1} can be assigned to the stretching vibration of Ti–O or Ti–O–Ti [26]. A broad and intense band in the region of 3200–3550 cm^{-1} can be ascribed to O–H stretching vibrations, existence of hydroxyl groups and huge amount of water molecules in the surface and interlayer space. The sharp peak at 1650 cm^{-1} confirmed the presence of water and can be assigned to H–O–H bending vibrations of water molecules.

SEM and TEM analysis

The morphology of the sample is characterized by SEM and TEM. Figure 3a shows the SEM image of the as-synthesized TNTs, it is indicated that the as-synthesized TNTs are interlaced each other. The nanotube length ranges from several tens to hundreds of nanometers. Figure 3b shows the TEM image of the as-synthesized TNTs, revealing large quantity of tubular materials with narrow size distribution. The tubes are central hollow and open ended. The inner diameter of the TNTs is found to be about 5–7 nm and outer diameter of 9–13 nm.

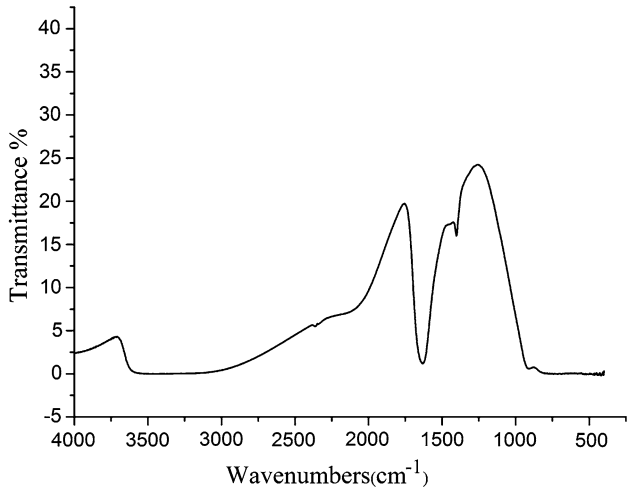

Fig. 2 FTIR spectra of TNTs

Kinetics of adsorption

The adsorption of Th(IV) on TNTs has been investigated as a function of contact time. As shown in Fig. 4, The amount of adsorbed Th(IV) soars with time increase, and equilibrium is maintained between two phases after about 8 h. The quick adsorption of Th(IV) suggests that chemical adsorption rather than physical adsorption contributes to Th(IV) adsorption on TNTs [10]. 12 h are enough to achieve the adsorption equilibrium in our experiments. In the subsequent experiments, the contact time of 12 h was fixed for adsorption equilibration of Th(IV) on TNTs. In order to investigate the mechanism of adsorption the kinetics of adsorption has to be studied, the pseudo-second-order rate equation was used to simulate the kinetic adsorption [27]:

$$\frac{t}{q_t} = \frac{1}{kq_e^2} + \frac{t}{q_e} \quad (3)$$

where k (g mg^{-1} min^{-1}) is the rate constant of the model, q_t (mg g^{-1}) is the amount of Th(IV) on TNTs at contact time t (min), q_e (mg g^{-1}) is the equilibrium adsorption capacity. Linear plot feature of (t q_t^{-1}) versus t is shown in Fig. 5. The data was fitted by the pseudo-second-order rate equation with $y = 0.0054X + 0.039$. The q_e and k values calculated from the slope and intercept were 185.18 mg g^{-1} and 7.47 $\times$ 10^{-4} g mg^{-1} min^{-1}, respectively. The regression coefficients ($R^2 = 0.99$) for the linear plot is very close to 1,

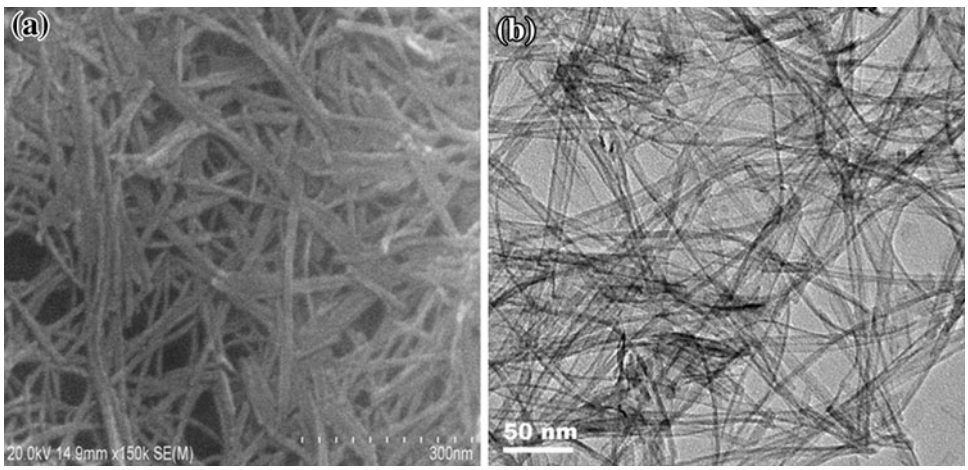

Fig. 3 SEM and TEM image of TNTs. **a** SEM; **b** TEM

which indicates that the experimental data can be described by the pseudo-second-order rate model well.

Effect of initial pH and ionic strength

Figure 6 shows the distribution of Th(IV) as a function of pH values in aqueous solution. We can see that, at pH $\leq$ 2.5, Th^{4+} is more than 70 %, $Th(OH)^{3+}$ is less than 30 %; at pH $\leq$ 3.0, Th^{4+} is less than 35 %, $Th(OH)^{3+}$ is less than 45 %, $Th(OH)_3^+$ and $Th(OH)_4$ is less than 0.3 %; at pH $\leq$ 4.0, Th^{4+} is less than 2 %, $Th(OH)^{3+}$ is less than 17 %, $Th(OH)_2^{2+}$ is less than 54 %, $Th(OH)_4$ and $Th(OH)_3^+$ is less than 14 %. At high pH values, $Th(OH)_4$(aq) could form $Th(OH)_4$ precipitation ($K_{sp} = 2 \times 10^{-45}$), which loses one or two water molecule to form $ThO(OH)_2$ ($K_{sp} = 5 \times 10^{-24}$) and ThO_2 precipitation. Östhols [28] found that $Th(OH)_3CO_3^-$ and $Th(CO_3)_5^{6-}$ can be negligible at pH range 2–4.5, while the hydrolysis products and the precipitation at pH > 4 must play an important role in the adsorption of Th(IV). Thereby, $Th(OH)_3CO_3^-$ and $Th(CO_3)_5^{6-}$ can be negligible at pH $\leq$ 3 in this experiments.

The adsorption of Th(IV) on TNTs in 0.01 mol L^{-1} $NaClO_4$ solution as a function of pH is shown in Fig. 7. Adsorption of Th(IV) is strongly dependent on pH values. Adsorption of Th(IV) increases at pH 1–4, and then maintains its maximum level with increasing pH values. The typical pH dependence adsorption was also found for the adsorption of Th(IV) on TiO_2 nanoparticles [13]. The variation of pH before and after adsorption was also measured. The pH values of the solution after adsorption changes a little to the acidic region, which indicates that H^+ is released during the adsorption. The adsorption of Th(IV) depends on the number of hydroxyl groups on TNTs surfaces and the concentration of hydroxyl groups is controlled by pH. At pH < 7, ≡ TiOH is the primary hydroxyl groups in TNTs [13, 22], and the Th^{4+},$Th(OH)^{3+}$ and $Th(OH)_2^{2+}$ is the predominating species in Th(IV) solution. The exchange reaction of metal cations with the hydroxyls on the surfaces is presumed as:

$$\equiv \mathrm{TiOH} + \mathrm{Th}^{4+} \rightarrow \equiv \mathrm{TiOTh}^{3+} + \mathrm{H}^+ \quad (4)$$

$$\equiv \mathrm{TiOH} + \mathrm{Th(OH)}_{4-n}^{n+} \rightarrow \equiv \mathrm{TiOTh(OH)}_{4-n}^{(n-1)+} + \mathrm{H}^+ \quad (5)$$

The positively charged Th^{4+}, $Th(OH)^{3+}$ and $Th(OH)_2^{2+}$ species in solution may exchange with −H from ≡TiOH groups of the hydrolyzed TNTs. The H^+ is released from TNTs to solution and thus the pH decreases after

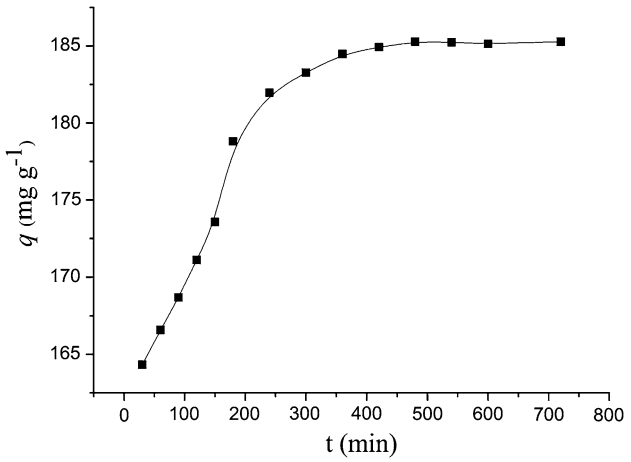

Fig. 4 Effect of contact time on Th(IV) adsorption rate onto TNTs (C_0(Th(IV)) = 0.2 mg mL^{-1}, m/V = 1 g L^{-1}, I = 0.01 mol L^{-1} $NaClO_4$, initial pH = 3 ± 0.1, T = 298.15 ± 2 K)

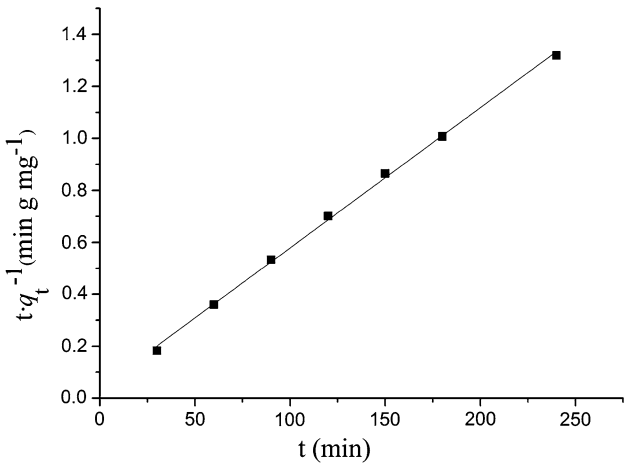

Fig. 5 Pseudo second order fits for the kinetic date corresponding onto Th(IV) adsorption on TNTs (C_0(Th(IV)) = 0.2 mg mL^{-1}, m/V = 1 g L^{-1}, I = 0.01 mol L^{-1} $NaClO_4$, initial pH = 3 ± 0.1, T = 298.15 ± 2 K)

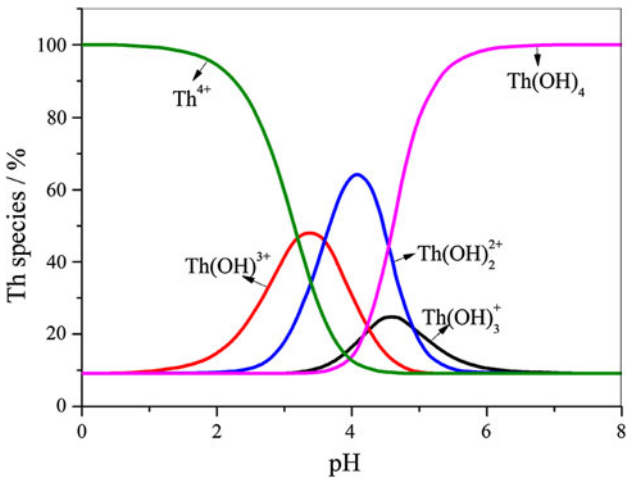

Fig. 6 The speciation of Th(IV) in aqueous solution

equilibration. Similar results were also reported for the adsorption of Eu(III) on TNTs [22].

The adsorption of Th(IV) on TNTs at pH 3.0 as a function of $NaClO_4$ concentrations is shown in Fig. 8. As can be seen that the adsorption of Th(IV) decreases a little with increasing $NaClO_4$ concentration. This suggests that Th(IV) adsorption is weakly dependent on ionic strength. The weakly dependence adsorption of Th(IV) onto TNTs on ionic strength and strongly dependence adsorption on pH values indicate that the adsorption mechanism of Th(IV) is chemical adsorption or surface complexation but ion exchange [6, 29]. In general, surface complexation is influenced by pH values, whereas ion exchange is mainly influenced by ionic strength [30, 31].

Adsorption isotherms

The adsorption isotherm is the equilibrium relationship between the concentration in the fluid phase and the concentration in the sorbent particles at a given temperature and pH. The adsorption isotherm parameters show actually the surface properties and affinity of the sorbent. Langmuir and Freundlich equations are the most frequently used for describing adsorption isotherms.

The Langmuir model assumes that there is no interaction between the adsorbate molecules and the adsorption is localized in a monolayer. The Freundlich equation is an empirical equation employed to describe the heterogeneous systems and is not restricted to the formation of the

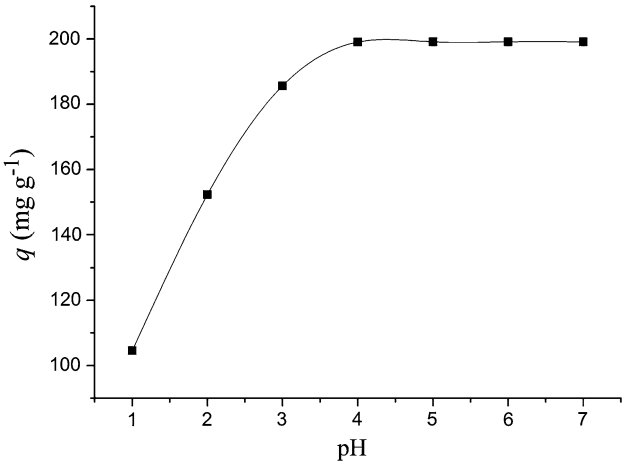

Fig. 7 Effect of pH on Th(IV) adsorption onto TNTs (C_0(Th(IV)) = 0.2 mg mL^{-1}, m/V = 1 g L^{-1}, I = 0.01 mol L^{-1} $NaClO_4$, T = 298.15 ± 2 K)

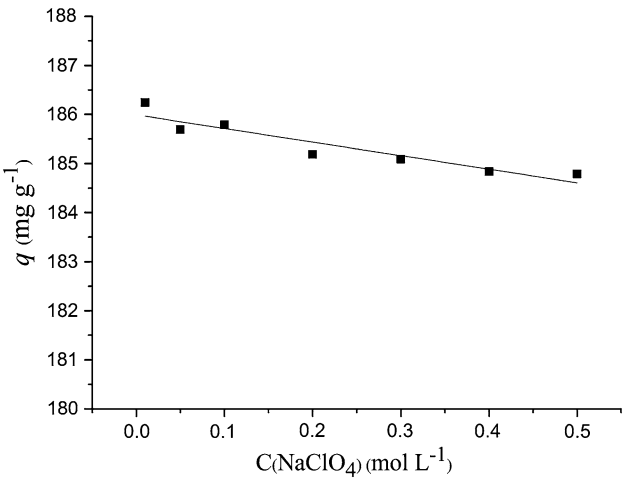

Fig. 8 Effect of ionic strength on Th(IV) adsorption onto TNTs (C_0(Th(IV)) = 0.2 mg mL^{-1}, m/V = 1 g L^{-1}, initial pH = 3 ± 0.1, T = 298.15 ± 2 K)

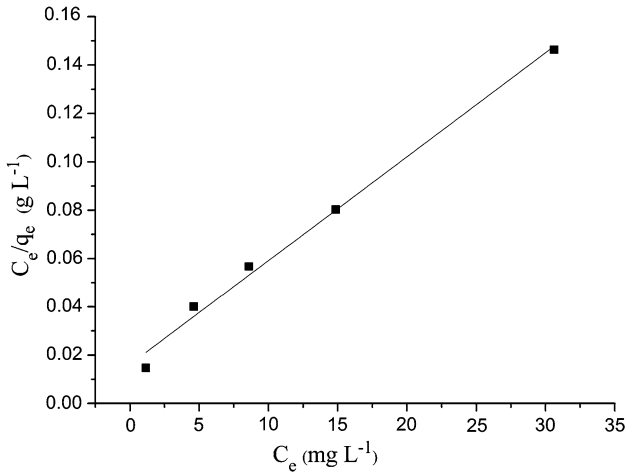

Fig. 9 Langmuir adsorption isotherm of Th(IV) on TNTs (C_0(Th(IV)) = 0.2 mg mL^{-1}, m/V = 1 g L^{-1}, I = 0.01 mol L^{-1} $NaClO_4$, initial pH = 3 ± 0.1, T = 298.15 ± 2 K)

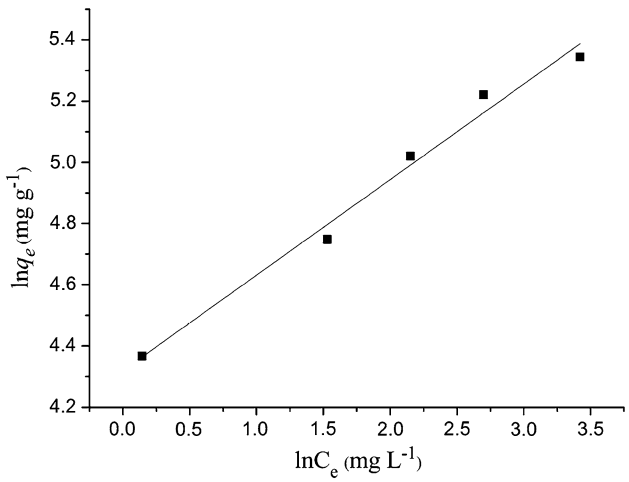

Fig. 10 Freundlich adsorption isotherm of Th(IV) on TNTs (C_0(Th(IV)) = 0.2 mg mL^{-1}, m/V = 1 g L^{-1}, I = 0.01 mol L^{-1} $NaClO_4$, initial pH = 3 ± 0.1, T = 298.15 ± 2 K)

monolayer. The form of Langmuir isotherm and Freundlich isotherm can be represented by the following equation [32, 33]:

$$\frac{C_e}{q_e} = \frac{C_e}{q_m} + \frac{1}{q_m b} \quad (6)$$

$$\ln q_e = \ln K_F + \frac{1}{n} \ln C_e \quad (7)$$

where q_m (mg g^{-1}) is the maximum adsorption capacity and b (L mg^{-1}) is the Langmuir adsorption constant that relates to the energy of adsorption; K_F (mg^{1-n} g^{-1} L^n) is the Freundlich constants which are indicators of adsorption capacity, and $1/n$ represents the degree of adsorption dependence at equilibrium concentration [34].

Figures 9 and 10 demonstrate the fitted resulting diagrams based on Langmuir and Freundlich equations. The slopes and intercepts of the linear Langmuir and Freundlich plots are used to calculate the Langmuir and Freundlich parameters were tabulated in Table 1. The value of R^2 showed that the adsorption isotherms are simulated by Langmuir and Freundlich models well. The value of $1/n$ indicates a favorable adsorption at $0 < 1/n < 1$. The $1/n$ value of the adsorption of Th(IV) on TNTs is 0.31, which indicates that the adsorption process can be easily taken place [29, 35, 36].

Process thermodynamic parameters

Temperature is an important parameter that dominates the physicochemical behavior of metal ions in the environment. Variation of standard thermodynamic parameters during the adsorption process was evaluated using the following equations [37]:

$$\ln K_d = \frac{\Delta S^\circ}{R} - \frac{\Delta H^\circ}{RT} \quad (8)$$

$$\Delta G^\circ = \Delta H^\circ - T\Delta S^\circ \quad (9)$$

where ΔS°, ΔH° and T are the standard entropy, standard enthalpy, and temperature in Kelvin, respectively, and R (8.314 J mol^{-1} K^{-1}) is the gas constant. Thermodynamic parameters (ΔG°, ΔH° and ΔS°) associated with the adsorption of Th(IV) on TNTs were calculated by using this plot of ln K_d versus $1/T$ and Eqs. (8) and (9). The values of thermodynamic parameters for the adsorption of Th(VI) at different temperature were given in Table 2. Table 2 reveals that the value of ΔH° is positive which shows that the adsorption of Th(IV) on TNTs is an endothermic process,and high temperature is advantageous for Th(IV) adsorption onto TNTs. One possible explanation to this positive enthalpy is that the adsorption of Th(IV) can be done in two process: first, the hydration shell surrounding of Th(IV) dehydration to form a single Th(IV) ion, this process needs energy; Then the adsorption of Th(IV) on TNTs by surface complexation, energy will be released in this process; The energy required for the former process exceeds the energy released in the later process, and therefore adsorptions become endothermic [8, 38].

The negative value of ΔG° shows that the adsorption of Th(IV) on TNTs is a spontaneous process. The value of ΔG° becomes more negative at higher temperature, which indicates that more efficient adsorption at higher temperature.

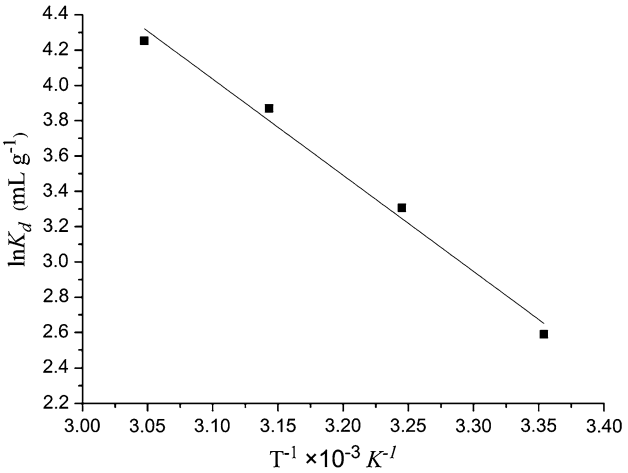

Fig. 11 The effect of solution temperaure on the distribution coefficient of Th(IV) on TNTs (C_0(Th(IV)) = 0.2 mg mL^{-1}, m/V = 1 g L^{-1}, I = 0.01 mol L^{-1} $NaClO_4$, initial pH = 3 ± 0.1)

Table 1 The parameters for the Langmuir and Freundlich model

Isotherms model	Parameters	
Langmuir	q_m (mg g^{-1})	232.56
	b (L mg^{-1})	0.27
	R^2	0.99
Freundlich	K_F (mg^{1-n} g^{-1} L^n)	75.15
	$1/n$	0.31
	R^2	0.98

Table 2 Thermodynamics parameters for Th(IV) adsorption onto TNTs

Sample	ΔH°/kJ mol^{-1} K^{-1}	ΔS°/J mol^{-1} K^{-1}	ΔG°/kJ mol^{-1}			
			298.15	308.15	318.15	328.15
TNTs	45.29	173.98	−6.58	−8.32	−10.06	−11.80

Conclusion

Analysis of the results revealed that the TNTs successfully synthesized under hydrothermal conditions of 150 °C. The adsorption of Th(IV) on TNTs is fast and rate of adsorption can be fitted well by pseudo-second-order kinetic model. The Langmuir isotherm model fits the adsorption data better than the Freundlich model. The adsorption of Th(IV) on TNTs is strongly dependent on pH values, but weakly dependent on ionic strength; The adsorption of Th(IV) on TNTs is an endothermic and a spontaneous process which becomes more favorable at higher temperature. Experimental results provide the evidence that the adsorption of Th(IV) on TNTs may be mainly attributed to chemical adsorption or surface complexation. The results of the experimental studies showed that TNTs have a high potential for application in the removal of Th(IV) from aqueous solution.

Acknowledgments Financial supports from National Natural Science Foundation of China (21203022; 21261001) is acknowledged.

References

1. Vearrier D, Curtis JA, Greenberg MI (2009) Technologically enhanced naturally occurring radioactive materials. Clin Toxicol 47:393–406
2. Höllriegla V, Greitera M, Giussania A et al (2007) Observation of changes in urinary excretion of thorium in humans following ingestion of a therapeutic soil. J Environ Radioact 95:149
3. Ueno K, Hoshi M (1970) The precipitation of some actinide element complex ions by using hexammine cobalt(III) cation–I: the precipitation of thorium and plutonium(IV) carbonate complex ions with hexammine cobalt(III) chloride. J Inorg Nucl Chem 32:3817–3822
4. Bayyari MA, Nazal MK, Khalili FA (2010) The effect of ionic strength on the extraction of Thorium(IV) from nitrate solution by didodecylphosphoric acid (HDDPA). J Saudi Chem Soc 14:311–315
5. Kiliari T, Pashalidis I (2011) Thorium determination in aqueous solutions after separation by ion-exchange and liquid extraction. J Radioanal Nucl Chem 288:753–758
6. Hu T, Tan LQ (2012) Modifying attapulgite clay by ammonium citrate tribasic for the removal of radionuclide Th(IV) from aqueous solution. J Radioanal Nucl Chem 292:819–827
7. Chen CL, Li XL, Wang XK (2007) Application of oxidized multi-wall carbon nanotubes for Th(IV) adsorption. Radiochim Acta 95:261–266
8. Wang MM, Tao XQ, Song XP (2011) Effect of pH, ionic strength and temperature on sorption characteristics of Th(IV) on oxidized multiwalled carbon nanotubes. J Radioanal Nucl Chem 288: 859–865
9. Gok C, Turkozu DA, Aytas S (2011) Removal of Th(IV) ions from aqueous solution using bi-functionalized algae-yeast biosorbent. J Radioanal Nucl Chem 287:533–541
10. Zuo LM, Yu SM, Zhou H et al (2011) Th(IV) adsorption on mesoporous molecular sieves: effects of contact time, solid content, pH, ionic strength, foreign ions and temperature. J Radioanal Nucl Chem 288:379–387
11. Guo GL, Luo MB, Xu JJ et al (2009) Separation and continuous determination of the light rare earth element and thorium in Baotou Iron Ore by a micro-column. J Radioanal Nucl Chem 281:647–651
12. Xu JZ, Fan QH, Bai HB, Wang DL et al (2009) Effects of Ionic Strength, Temperature and Humic Substances Concentration on the Sorption of Th(IV) to Attapulgite. J Nucl Radiochem 31:179–185
13. Tan XL, Wang XK, Fang M et al (2007) Sorption and desorption of Th(IV) on nanoparticles of anatase studied by batch and spectroscopy methods. Colloids Surf A 296:109–116
14. Anirudhan TS, Bringle CD, Rijith S (2010) Removal of uranium(VI) from aqueous solutions and nuclear industry effluents using humic acid-immobilized zirconium-pillared clay. J Environ Radioact 101:267–276
15. Chen Q, Peng LM (2007) Structure and applications of titanate and related nanostructures. Int J Nanotechnol 4:44–65
16. Liu SS, Lee CK, Chen HC et al (2009) Application of titanate nanotubes for Cu(II) ions adsorptive removal from aqueous solution. Chem Eng J 147:188–193
17. An HQ, Zhu BL, Wu HY et al (2008) Synthesis and characterization of titanate and CS_2-modified titanate nanotubes as well as their adsorption capacities for heavy metal ions. Chem J Chin U 29:439–444
18. Chen YC, Lo SL, Kuo J (2010) Pb(II) adsorption capacity and behavior of titanate nanotubes made by microwave hydrothermal method. Colloids Surf A 361:126–131
19. Wang T, Liu W, Xiong L et al (2013) Influence of pH, ionic strength and humic acid on competitive adsorption of Pb(II), Cd(II) and Cr(III) onto titanate nanotubes. Chem Eng J 215–216:366–374
20. Niu HY, Wang JM, Shi YL et al (2009) Adsorption behavior of arsenic onto protonated titanate nanotubes prepared via hydrothermal method. Micro Macro Mater 122:28–35
21. Chang Y, Zhang LX, Luo MB et al (2010) Synthesis and Adsorptive Removal for Uranium(VI) Ions of Titanate Nanotubes. Chinese J Mater Res 24:424–428
22. Sheng GD, Yang ST, Zhao DL et al (2012) Adsorption of Eu(III) on titanate nanotubes studied by a combination of batch and EXAFS technique. Sci China Chem 42:60–73
23. Sheng GD, Yang ST, Sheng J et al (2011) Influence of solution chemistry on the removal of Ni(II) from aqueous solution to titanate nanotubes. Chem Eng J 168:178–182
24. Suetake J, Nosaka AY, Hodouchi K et al (2008) Characteristics of titanate nanotube and the states of the confined so dium ions. J Phys Chem C 112:18474–18482
25. Lin KS, Cheng HW, Chen WR et al (2010) Synthesis, characterization, and adsorption kinetics of titania nanotubes for basic dye wastewater treatment. Adsorption 16:47–56
26. Rodrigues CM, Ferreira OP, Alves OL (2010) Interaction of sodium titanate nanotubes with organic acids and base: chemical, structural and morphological stabilities. J Braz Chem Soc 21:1–8
27. Ho YS, McKay G (1999) Pseudo-second order model for sorption processes. Process Biochem 34:451–465
28. Östhols E (1995) Thorium sorption on amorphous silica. Geochim Cosmochim Acta 59:1235–1249
29. Lu SS, Guo ZQ, Zhang CC et al (2011) Sorption of Th(IV) on MX-80 bentonite: effect of pH and modeling. J Radioanal Nucl Chem 287:621–628
30. Baeyens B, Bradbury MH (1997) A mechanistic description of Ni and Zn adsorption on Na-montmorillonite. Part I: titration and sorption measurements. J Contam Hydro 27:199–222
31. Wang XK, Chen CL, Du JZ et al (2005) Effect of pH and aging time on the kinetic dissociation of ^{243}Am(III) from humic acid coated γ-Al_2O_3: a chelating resin exchange study. Environ Sci Technol 39:70–84

32. Langmuir I (1916) The constitution and fundamental properties of solids and liquids. J Am Chem Soc 38:2221–2295
33. Freundlich HMF (1906) Überdie adsorption in lösungen. Z Physikalische Chem (Leipzig) 57A:385–470
34. Saberi R, Nilchi A, Rasouli Garmarodi S et al (2010) Adsorption characteristic of ^{137}Cs from aqueous solution using PAN-based sodium titanosilicate composite. J Radioanal Nucl Chem 284:461–469
35. Zeng YH, Liao XP, He Q et al (2009) Recovery of Th(IV) from aqueous solution by reassembled collagen-tannin fiber adsorbent. J Radioanal Nucl Chem 280:91–98
36. Anirudhan TS, Rejeena SR (2011) Thorium(IV) removal and recovery from aqueous solutions using tannin-modified poly (glycidylmethacrylate)-grafted zirconium oxide densified cellulose. Ind Eng Chem Res 50:13288–13298
37. Kilislioglu A, Bilgin B (2003) Thermodynamic and kinetic investigations of uranium adsorption on amberlite IR-118H resin. Appl radiat isotopes 58:155–160
38. Shirvani M, Shaiatmadari H, Kalbasi M et al (2006) Sorption of cadmium on palygorskite, sepiolite and calcite: equilibria and organic ligand affected kinetics. Colloids Surf A 287:182–190